

# Long non-coding ribonucleic acid urothelial carcinoma-associated 1 promotes high glucose-induced human retinal endothelial cells angiogenesis through regulating micro-ribonucleic acid-624-3p/vascular endothelial growth factor C

Huang Yan<sup>1,†</sup>, Panpan Yao<sup>2,†</sup>, Ke Hu<sup>3,\*</sup> , Xueyao Li<sup>1</sup>, Hong Li<sup>3</sup>

<sup>1</sup>Ophthalmology Department, Chongqing Yubei District People's Hospital, Chongqing, China, <sup>2</sup>Department of Ophthalmology, Changzheng Hospital, Naval Medical University, Shanghai, China, and <sup>3</sup>Ophthalmology Department, the First Affiliated Hospital of Chongqing Medical University, Chongqing, China

## Keywords

Angiogenesis, Diabetic retinopathy, Urothelial carcinoma-associated 1

## \*Correspondence

Ke Hu

Tel.: +023-61800285

Fax: +023-61800285

E-mail address:

qwazdxc246@163.com

*J Diabetes Investig* 2021; 12: 1948–1957

doi:10.1111/jdi.13617

## ABSTRACT

**Aims/Introduction:** Emerging evidence has indicated that long non-coding ribonucleic acids play important roles in the development and progression of diabetic retinopathy (DR). It is reported that urothelial carcinoma-associated 1 (UCA1) is highly expressed in diabetic lymphoendothelial cells and influences glucose metabolism in rats with DR. The aim of the present study was to explore the role of UCA1 in the mechanism of DR.

**Materials and Methods:** Gene expression analyses in fibrovascular membranes excised from patients with DR using public microarray datasets (GSE60436). Reverse transcription polymerase chain reaction was carried out to detect UCA1, micro-ribonucleic acid (miR)-624-3p and vascular endothelial growth factor C (VEGF-C) expressions in the blood of patients and human retinal endothelial cells (HRECs). Furthermore, Cell Counting kit-8, Transwell assay, and tube formation assay were used to identify biological effects of UCA1 on HRECs proliferation, migration ability and angiogenesis *in vitro*.

**Results:** UCA1 and VEGF-C were elevated in DR patients and high glucose-induced HRECs cell lines, whereas miR-624-3p was decreased. UCA1 inhibition inhibited proliferation, angiogenesis and migration of HRECs cells under high-glucose condition. Luciferase reporter assay showed that UCA1 could sponge with miR-624-3p, which could directly target VEGF-C. Finally, we proved a pathway that UCA1 promoted cell proliferation, migration and angiogenesis through sponging with miR-624-3p, thereby upregulating VEGF-C in high-glucose-induced HRECs.

**Conclusions:** We identified UCA1 as an important factor associated with DR, which could regulate the expression of VEGF-C by sponging miR-624-3p in human retinal endothelial cells. Our results pave the way for further studies on diagnostic and therapeutic studies related to UCA1 in DR patients.

## INTRODUCTION

Diabetic retinopathy (DR) is a leading cause of visual impairment and blindness worldwide<sup>1</sup>. Emerging evidence shows that

DR is characterized by changes in retinal microvessel function and integrity induced by hyperglycemia, which leads to progressive retinal ischemia and angiogenesis<sup>2,3</sup>. Vascular endothelial growth factor (VEGF) is considered to be the main factor involved in angiogenesis<sup>4,5</sup>, and the side-effects can be reduced

<sup>†</sup>Both authors contributed equally to this work.

Received 10 October 2020; revised 20 May 2021; accepted 26 May 2021

and the effectiveness of the treatment can be improved when combined with anti-VEGF therapy<sup>6,7</sup>. VEGF-C is a soluble member of the VEGF family, and the role of VEGF-C in neovascularization is supported by the fact that exogenous VEGF-C could recover lymphatic vascularization through stimulating neolymphangiogenesis<sup>8</sup>. Furthermore, VEGF-C also participates in the laser-induced choroidal neovascularization formation in Brown Norway rats<sup>9</sup>. High expression of VEGF-C has been shown in proliferative DR<sup>10</sup>. However, the specific role of VEGF-C in the pathogenesis of DR is unclear.

It is known that long non-coding ribonucleic acids (lncRNAs) are important regulators of gene expression in diverse types of tissues, as well as different diseases<sup>11,12</sup>. Several studies have shown that VEGF-C binds to lncRNAs, and can function as an important downstream regulator in cancer development and progress<sup>13,14</sup>. Long non-coding RNA urothelial carcinoma-associated 1 (UCA1) was first found to be upregulated in bladder cancer<sup>15</sup>. Later studies also found that high expression of UCA1 was associated with various cancers, and UCA1 can stimulate the proliferation, migration and epithelial–mesenchymal transformation of tumor cells<sup>16–18</sup>. It is reported that UCA1 is highly expressed in diabetic lymphoendothelial cells<sup>19</sup>, and influences glucose metabolism in rats with diabetic nephropathy<sup>20</sup>. It is currently undetermined whether UCA1 affects the expression of VEGF-C in DR development.

We recently profiled the gene expression patterns associated with DR in fibrovascular membranes, and found that UCA1 is one of the most highly upregulated genes in DR patients when compared with controls. Furthermore, UCA1 was upregulated in both the blood of DR patients and high-glucose-treated HRECs. Increasing evidence has revealed the functions of lncRNAs as microRNA (miRNA) sponges in various diseases, including diabetes, cancer, atherosclerosis, metabolic syndrome and aging<sup>21,22</sup>. As previously reported, lncRNA UCA1 might interact with several types of miRNAs (Table S1). Through open-source miRNA target prediction software (TargetScan

Software), we found that 3'-UTR of microRNA (miR)-624-3p contained a putative binding site for lncRNA UCA1, indicating it might be a direct target for the lncRNA. Furthermore, we also observed a putative binding site for miR-624-3p in the 3'-UTR region of VEGF-C messenger RNA. In addition, VEGF-C controls angiogenesis in chondrosarcoma through regulating the expression of miR-624-3p<sup>23</sup>. We therefore hypothesize that UCA1 might serve as a miRNA sponge to regulate VEGF-C expression through binding to miR-624-3p. Our *in vitro* study implies that the UCA1–miR-624-3p–VEGF-C axis plays a crucial role in the mechanism of DR. UCA1 might be a promising therapeutic target for DR treatment.

## MATERIALS AND METHODS

### Clinical data

Blood samples were collected from the Ophthalmology Department, Chongqing Yubei District People's Hospital (Chongqing, China), between December 2018 and November 2019. All the samples were immediately centrifuged and kept at  $-80^{\circ}\text{C}$  for the following experiments. Candidates included 50 persons with clinically detected DR, 50 patients with type 2 diabetes, and 50 individuals who were free from DR and type 2 diabetes. The characteristics of the patients and normal volunteers are shown in Table 1. The present study received approval from the Institutional Ethics Review Board of Chongqing Yubei District People's hospital. The ethical record number was 20186183 and the approval date was 18 June 2018.

### Cell culture

Human retinal endothelial cells (HRECs) were purchased from ScienCell company (San Diego, CA, USA). HRECs were cultured in a human endothelial medium (Sciencell, Carlsbad, CA, USA) according to the instructions. The medium was supplemented with 5% fetal bovine serum (Sangon Biotech Co., Ltd., Shanghai, China) and 100  $\mu\text{g}/\text{mL}$  streptomycin (Sangon Biotech Co., Ltd.). All the cells were divided into a 5 mmol/L

**Table 1** | Baseline characteristics of the participants

	DR <i>n</i> = 50	T2DM <i>n</i> = 50	Controls <i>n</i> = 50
Age (years)	58.12 $\pm$ 6.44	60.13 $\pm$ 5.89	59.64 $\pm$ 6.96
Sex ratio (male/female)	23/25	25/25	24/26
HbA1c (%)	8.29 $\pm$ 0.44 <sup>a</sup>	8.01 $\pm$ 1.02 <sup>b</sup>	5.30 $\pm$ 0.55
BP (mmHg)			
Systolic	123.60 $\pm$ 4.48	125.34 $\pm$ 3.78	122.42 $\pm$ 4.01
Diastolic	82.06 $\pm$ 4.46	81.01 $\pm$ 3.98	82.74 $\pm$ 4.83
FPG (mg/dL)	7.76 $\pm$ 0.45 <sup>c</sup>	7.40 $\pm$ 0.55 <sup>d</sup>	5.01 $\pm$ 0.71
BMI (kg/m <sup>2</sup> )	32.04 $\pm$ 2.06 <sup>e</sup>	33.10 $\pm$ 1.19 <sup>f</sup>	24.92 $\pm$ 1.50
Duration of diabetes (years)	20.60 $\pm$ 0.60 <sup>g</sup>	18.40 $\pm$ 1.20	–

<sup>a</sup>*P* < 0.01 vs controls, <sup>b</sup>*P* < 0.01 versus controls, <sup>c</sup>*P* < 0.01 versus controls, <sup>d</sup>*P* < 0.01 versus controls, <sup>e</sup>*P* < 0.01 versus controls, <sup>f</sup>*P* < 0.01 versus controls, <sup>g</sup>*P* < 0.05 versus type 2 diabetes (T2DM). BMI, body mass index; BP, blood pressure; DR, diabetes retinopathy; FPG, fasting plasma glucose; HbA1c, glycated hemoglobin.

glucose group and a 25 mmol/L glucose group, and maintained at 37°C in a humidified 5% CO<sub>2</sub> incubator.

#### Lactate dehydrogenase assay

Lactate dehydrogenase (LDH) activities in the supernatant of cell homogenate and the medium were measured using the Cytotoxicity Detection Kit (Roche Applied Science, Basel, Switzerland) according to the manufacturer's instructions. Absorbance at 490 nm was measured by a microplate reader (Bio-Tek, Winooski, VT, USA). The percentage leakage of LDH was calculated as (LDH activity in medium / [LDH activity in medium + LDH activity in cells]) × 100%. Assays were repeated in triplicate.

#### Plasmid constructs

The UCA1 overexpression vector (pcDNA-UCA1) and negative control empty vector were commercially constructed by GenePharma (Shanghai, China). A Fast Site-Directed Mutagenesis Kit (Tiangen Biotech, Beijing, China) was used to mutate the miRNA binding sites in the UCA1 sequence. All of the constructs were confirmed by sequencing.

#### RNA immunoprecipitation and RNA pull-down assays

Magna RIP RNA-Binding Protein Immunoprecipitation Kit (Millipore, Billerica, MA, USA) was used to carry out RNA immunoprecipitation (RIP) experiments according to the manufacturer's instructions. RNA pull-down assay was carried out using the RNA Pull-Down Kit (Thermo Scientific Pierce, Waltham, MA, USA). AGO<sub>2</sub> antibody (Cell Signaling Technology, Shanghai, China) was utilized to verify the co-precipitated RNA, and normal mouse immunoglobulin G (Cell Signaling Technology) was used as the control. The RNAs in the immunoprecipitates were isolated with Trizol reagent and subjected to quantitative reverse transcription polymerase chain reaction (qRT-PCR) analysis, and the precipitated proteins were applied for western blot analysis.

#### Dual-luciferase reporter assay

The wild-type and mutant sequences of UCA1 and VEGF-C sequence were constructed into plasmids (Sangon Biotech Co., Ltd.). Cells were each seeded in 96-well plates with a density of  $4 \times 10^3$  cells per well. Then, luciferase vector and firefly luciferase plasmids were transfected into cells for 12 h; then, indicated wild-type and mutant sequences were each transfected into the prepared cells for 24 h. The luciferase activities were measured using a luciferase assay system (Beyotime, Shanghai, China) according to the manufacturer's protocols.

#### Cell proliferation assay

The cell proliferative activity was measured using the Cell Counting Kit-8 (CCK-8) assay (Sangon Biotech Co., Ltd.) according to the manufacturer's protocol. Approximately  $3 \times 10^3$  cells from each group were seeded into 96-well plates. When the cells attached down to the bottom of the plate, they

were starved for another 24 h in a serum-free medium. For each well, 10 μL of CCK-8 reagent was added, and incubated for 2 h. Then, the absorbance value was detected at a 450 nm with a microplate reader (Thermo Scientific Inc., Shanghai, China).

#### Cell migration assay

Cell migration was assayed in 24-well Transwell chambers with 8-μm pore size filter membrane (Corning, Shanghai, China). On reaching 90% confluence in plates, cells were treated with serum-free medium for 12 h. After removing the medium and floating cells, the cells were washed three times with sterile 1× phosphate-buffered saline and then stained with hematoxylin-eosin. The number of cells that migrated to the bottom side of the insert was counted under a microscope.

#### Tube formation assay

Capillary-like tube formation assay was carried out to investigate the tube formation capacity of HRECs. The frozen Matrigel (BD Biosciences, Shanghai, China) was thawed in a refrigerator at 4°C overnight and was then added to a pre-cooled 96-well plate. When the Matrigel solidified in a humidified 5% CO<sub>2</sub> incubator at 37°C, cells were seeded on Matrigel immediately at a density of  $7 \times 10^3$  cells per well. The plates were incubated in humidified 5% CO<sub>2</sub> at 37°C for 8 h. The following parameters were used for quantification. Tubes were considered to be a tubular structure that goes from one branching point to another branching point or to a loose end. Loops were enclosed (or almost enclosed) areas inside the tubes that fulfill roundness conditions. The images of the tubular network were captured by microscopy, and the quantification of capillaries was assessed using ImageJ software (NIH, Bethesda, MD, USA).

#### Western blot analysis

RIP assay buffer (Sangon Biotech Co., Ltd.) was used to extract proteins from cultured cells, and the concentration was determined using a bicinchoninic acid kit (Sangon Biotech Co., Ltd.). Proteins were resolved by 12% sodium dodecyl sulphate polyacrylamide gel electrophoresis. The proteins were transferred onto polyvinylidene difluoride membranes. Then, 10% milk was used to block the membranes at room temperature for 1 h. The membranes were then incubated with the appropriate primary antibody (Abcam, Cambridge, MA, USA) at 4°C overnight and secondary antibodies at room temperature for 2 h. The immunoreactive bands were visualized by enhanced chemiluminescence and normalized to glyceraldehyde-3-phosphate dehydrogenase.

#### Real-time RT-PCR

PrimeScript™ RT reagent Kit (TaKaRa, Shanghai, China) was used to reverse transcribe complementary deoxyribonucleic acid from total RNA, following the manufacturer's instructions. Quantitative gene expression was carried out using the Roche

LightCycler 480 (Roche, Penzberg, Germany). Relative RNA expression was calculated by the  $2^{-\Delta\Delta CT}$  method and normalized to glyceraldehyde-3-phosphate dehydrogenase. All quantitative PCRs were carried out in triplicate.

### Microarray analysis

Microarray expression profiles (GSE60436) were used for gene expression profiles, which can be obtained from the NCBI-GEO database. The Benjamini and Hochberg procedure was used to identify differences in gene profiles. RNAs with a fold-change  $\geq 2.0$  and a  $P$ -value  $< 0.05$  in the microarray data were considered significantly differentially expressed. Hierarchical clustering was carried out, and volcano plots were obtained to test whether the two types of samples were distinguishable. All analyses were carried out using the R 3.2.3 software package (The R Foundation for Statistical Computing, Vienna, Austria).

### Statistical analysis

All statistical analyses were carried out by using SPSS v20.0 (SPSS Inc, Chicago, IL, USA). Data are represented as the mean  $\pm$  standard deviation. Statistical significance between groups was determined using Student's  $t$ -test or the one-way ANOVA method.  $P < 0.05$  was considered to be statistically significant.

## RESULTS

### UCA1 is upregulated in DR patients and high-glucose-induced HRECs

To identify genes associated with the pathogenesis of DR, we carried out gene expression analyses in fibrovascular membranes excised from patients with DR and controls using public microarray datasets (GSE60436). To visualize the gene profile dataset, we generated a heatmap and volcano plot (Figure 1a,b), which could significantly discriminate the differentially expressed genes between DR samples and normal samples. In DR samples, we identified 766 significantly differentially expressed genes ( $P < 0.05$  and  $|\log_2 FC| \geq 1$ ). Of these genes, 448 genes were upregulated and 218 genes were downregulated. UCA1 was one of the most upregulated genes, which had 3.87 log<sub>2</sub> fold change.

Then, we detected the expression of UCA1 in the plasma from 50 DR patients, 50 type 2 diabetes patients and 50 healthy people by RT-PCR. The baseline characteristics of the participants included in the study are shown in Table 1. It is worth mentioning that the mean duration of diabetes was shorter in type 2 diabetes patients compared with DR patients ( $18.40 \pm 1.20$  vs  $20.6 \pm 0.60$  years;  $P = 0.039$ ). RT-PCR results showed that UCA1 was elevated in DR patients compared with type 2 diabetes patients, and type 2 diabetes patients had a higher level of UCA1 than healthy people (Figure 1c). We also found that VEGF-C was much higher and miR-624-3p was much lower (Figure 1d,e). Furthermore, we found that the expressions of UCA1 and VEGF-C in high-glucose-induced HRECs were significantly increased and miR-624-3p is downregulated (Figure 1f). It is worth noting that the expression of other VEGF subtypes (VEGF-A, VEGF-B, VEGF-D, VEGF-E,

VEGF-F and placental growth factor) was not significantly different between high-glucose-induced HRECs treated with small interfering group ((si)-UCA1) and without small interfering group (si-NC) (Figure S1), respectively.

### UCA1 promotes high-glucose-induced cell proliferation, migration and angiogenesis

LDH is a cytoplasmic enzyme that is rapidly released into the surrounding medium on cell damage. As shown in Figure 2a, no significant differences in the LDH activities were observed in cells of the si-UCA1 group and the si-NC group. The interference efficiency of UCA1 siRNA was determined through qRT-PCR. As shown in Figure 2b, the expression of UCA1 was significantly reduced in the si-UCA1 group compared with the si-NC group. To examine the proliferative ability of HRECs, the CCK-8 assay was carried out. The results showed that the si-NC group significantly increased the proliferation of HRECs compared with the si-UCA1 group, and the proliferation of HRECs induced by 25 mmol/L glucose was increased compared with HRECs treated with 5 mmol/L glucose. (Figure 2c). The migration ability of HRECs cells was determined by Transwell assays. As shown in Figure 2d, cell migration was significantly improved in the si-NC group compared with the si-UCA1 group. Similarly, the migration capacity of HRECs induced by 25 mmol/L glucose was significantly increased compared with HRECs treated with 5 mmol/L glucose. To explore whether UCA1 had an effect on angiogenesis, the tube formation of HRECs was evaluated by Matrigel assay. It was found that the number of capillary-like structures in the 25 mmol/L glucose group was significantly increased compared with that in the 5 mmol/L glucose group. In addition, the si-UCA1 group had fewer capillary-like structures compared with the si-NC group (Figure 2e).

### MiR-624-3p served as a target of UCA1

To confirm whether UCA1 regulates the expression of miR-624-3p through the predicted UCA1 binding sites, a dual-luciferase assay was carried out. The results show that UCA1 binds to miR-624-3p with high binding affinity. Compared with the miR-NC, miR-624-3p could significantly decrease wild-type UCA1 luciferase reporter activity, but no significant change in luciferase activity was observed after the binding sites were mutant (Figure 3a). As an important component of RNA-induced silencing complex, Argonaute 2 plays a key role in miRNAs inducing post-transcriptional regulation for the target genes<sup>24</sup>. To further explore associations between UCA1 and miR-624-3p, we carried out RIP and pull-down experiments. The pull-down experiments showed that the anti-Argonaute 2 antibody significantly enriched UCA1 (Figure 3b). The RIP results show that the production precipitated by anti-Argonaute 2 significantly enrich UCA1 in wild-type UCA1 HRECs when miR-624-3p was overexpressed (Figure 3c). To verify whether UCA1 was involved in the expression regulation of miR-624-3p, we overexpressed or knocked down UCA1 in

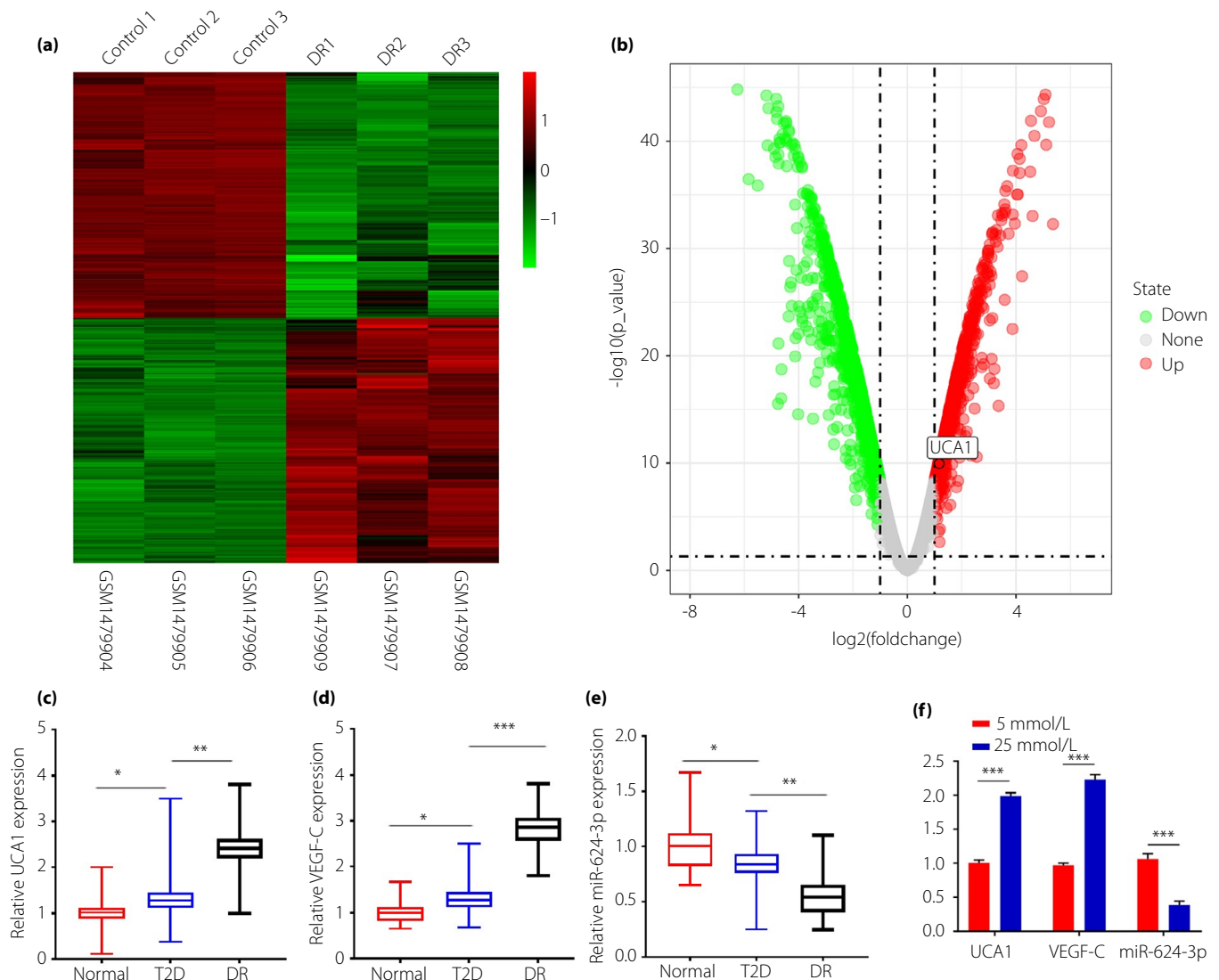


**Figure 1** | Identification of urothelial carcinoma-associated 1 (UCA1), miR-624-3p and vascular endothelial growth factor C (VEGF-C) in diabetic retinopathy (DR) and human retinal endothelial cells. (a) Clustered heatmap of the differentially expressed genes in DR. Upregulated genes are shown in red and downregulated genes are shown in green. (b) Volcano plots comparing gene expression between DR patients and controls. The red dots represent the significantly differentially expressed genes ( $|\log_{2}FC| > 1$  and  $P < 0.05$ ). (c–e) Reverse transcription polymerase chain reaction was used to detect UCA1, VEGF-C and miR-624-3p levels in blood from DR patients ( $n = 50$ ), type 2 diabetes (T2D) patients ( $n = 50$ ) and non-DR individuals ( $n = 50$ ). (f) Reverse transcription polymerase chain reaction was carried out to measure the expression level of UCA1, VEGF-C and micro-ribonucleic acid (miR)-624-3p in human retinal endothelial cells treated with 5 mmol/L or 25 mmol/L glucose for 48 h. All values represent the mean  $\pm$  standard deviation. \* $P < 0.05$ , \*\* $P < 0.01$ , \*\*\* $P < 0.001$ .

HRECs. It was found that miR-624-3p expression was significantly upregulated after UCA1 knockdown, whereas downregulated after overexpression of UCA1 (Figure 3d).

#### **UCA1 regulates high-glucose-induced cell proliferation, migration and angiogenesis through miR-624-3p/VEGF-C pathway**

Combining the bioinformatics method TargetScan, we identified VEGF-C as a possible downstream gene of miR-624-3p. The dual-luciferase assay shows that high binding affinity exists

between UCA1 and miR-624-3p. Furthermore, miR-624-3p could inhibit luciferase reporter activity and the inhibition effect disappeared after binding site mutation (Figure 4a). Thus, we hypothesized that UCA1 regulates high-glucose-induced cell proliferation, migration and angiogenesis through the miR-624-3p–VEGF-C pathway. To test this hypothesis, we transfected the miR-624-3p inhibitor into HRECs with si-UCA1 or si-NC after the cells had been treated with high glucose (25 mmol/L) or low glucose (5 mmol/L) for 48 h. The results show that the si-NC group significantly increased the expression of VEGF-C

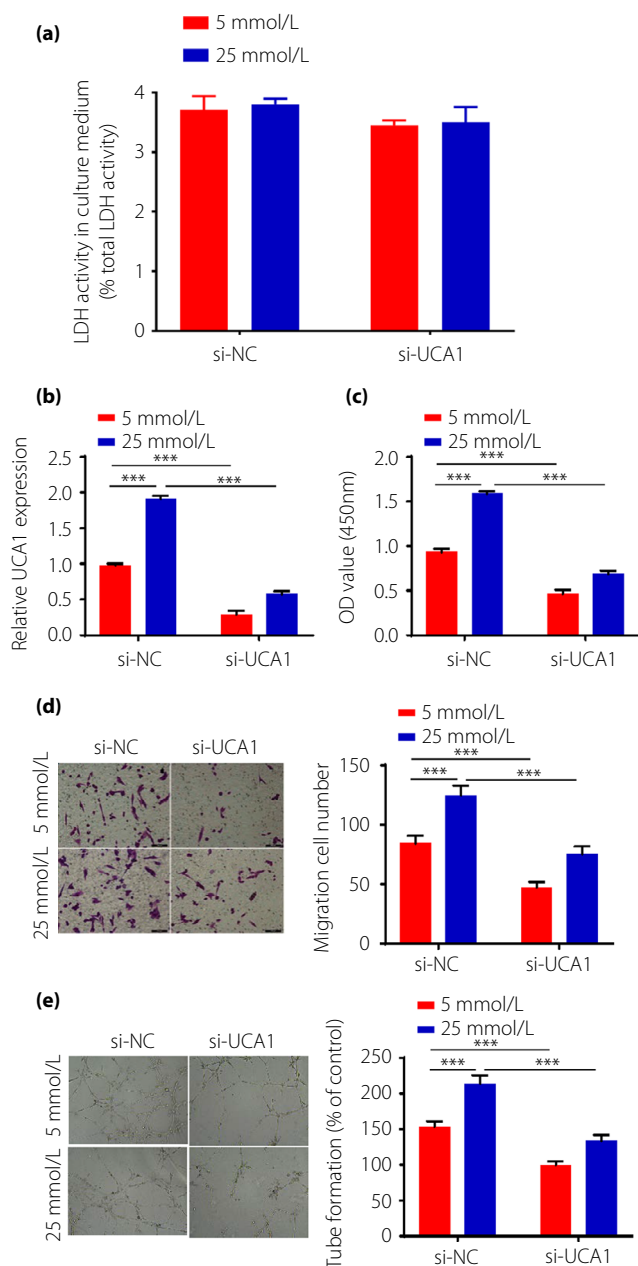


**Figure 2** | Urothelial carcinoma-associated 1 (UCA1) promotes high-glucose-induced cell proliferation, migration and angiogenesis. (a) Lactate dehydrogenase (LDH) analysis of human retinal endothelial cells of small interfering si-UCA1 group and si-NC group, (b) UCA1 expressions were detected by reverse transcription polymerase chain reaction. (c) Proliferation abilities of human retinal endothelial cells by Cell Counting Kit-8 assay. (d) Migration abilities were measured by Transwell assay. (e) Tube formation assay was carried out to detect the angiogenesis ability of human retinal endothelial cells. si-UCA1: small RNA interfering group; si-NC: without small interfering group; \*\*\* $p < 0.001$ .

compared with the si-UCA1 group, and the repressed VEGF-C in the si-UCA1 group was increased following miR-624-3p inhibitor or overexpression (oe)VEGF-C transfection (Figure 4b,c). Furthermore, CCK-8 assay showed that the repressed cell proliferation capacity in the si-UCA1 group was increased following miR-624-3p inhibitor or oeVEGF-C transfection (Figure 4d). In addition, Transwell assay showed that the repressed migration in si-UCA1 was reversed following miR-624-3p inhibitor or oeVEGF-C transfection (Figure 4e). In addition, tube formation assay showed that the repressed angiogenesis in the si-UCA1 group was promoted following miR-624-3p inhibitor or oeVEGF-C transfection (Figure 4f).

## DISCUSSION

The reason for the development of DR is mainly attributed to the increase of glucose levels, which unavoidably causes cellular stress and promotes the damage of vascular endothelial cells, leading to the abnormal development of capillaries<sup>25</sup>. Vascular endothelial involvement in vasomotor regulation and its dysfunction is suggested to play a pivotal role in the development of DR<sup>26</sup>. HRECs under high-glucose condition can mimic the pathogenesis of DR. High-glucose treatment has also been reported to enhance the proliferation, migration and tube formation of HRECs *in vitro*<sup>27,28</sup>. In the present study, we again showed the effects of high-glucose treatment on HRECs, and the results were consistent with previous studies.

LncRNAs are emerging as critical regulators that impact a variety biological functions and the pathogenesis of diseases<sup>29,30</sup>. Many studies have confirmed that lncRNAs are associated with the proliferation, migration and angiogenesis of HRECs<sup>31,32</sup>, and the abnormal expression of lncRNAs has been observed to be correlated with pathogenesis and progression of DR<sup>33,34</sup>. For example, lncRNA HOXA transcript at the distal tip improves diabetic retinal microangiopathy through the p38 mitogen-activated protein kinase pathway<sup>35</sup>. Overexpression of lncRNA maternally expressed 3 can inhibit the development of diabetic retinopathy by regulating transforming growth factor- $\beta$ 1<sup>36</sup>. Here, we identified a novel effect molecule on diabetic retinopathy, UCA1, which is upregulated in fibrovascular membranes excised from patients with DR. We also found that the expression level of UCA1 in plasma from DR patients was much higher than that of type 2 diabetes patients, and the latter was higher when compared with healthy individuals. Based on these studies, we hypothesize that UCA1 has important value for the study of DR.

Previous studies showed that DR was closely associated with the retinal microvascular system damage, and persistent high-glucose environment-caused retinal microvascular damage contributes to the development of DR<sup>25</sup>. Therefore, as an initial step toward characterizing the retinal damage effects of UCA1 during DR, we examined whether UCA1 can cause HRECs angiogenesis under normal glucose treatment conditions. As expected, UCA1 significantly induced cell proliferation, migration and tube formation, suggesting its involvement in retinal

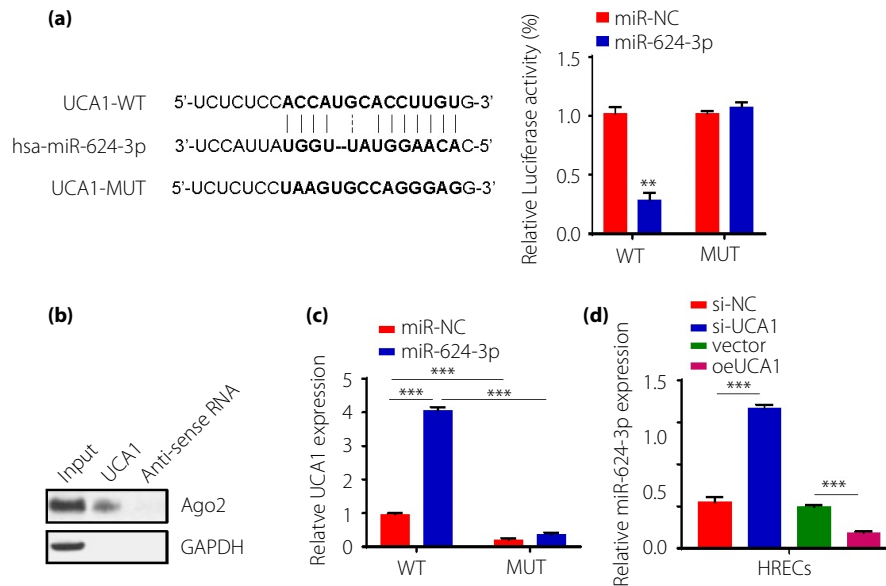


**Figure 3** | Urothelial carcinoma-associated 1 (UCA1) acted as a sponge of miR-624-3p. (a) Predicted miR-624-3p binding sites in UCA1 and luciferase assays in wild-type (WT)-UCA1 or mutant (MUT)-UCA1 human retinal endothelial cells co-transfected with micro-ribonucleic acid (miR)-NC or miR-624-3p. (b) The pull-down experiments show that the anti-Argonaute 2 (AGO2) antibody significantly enriched UCA1. (c) The enrichment of UCA1 in ribonucleic acid (RNA) immunoprecipitation. (d) miR-624-3p expression in human retinal endothelial cells transfected with small interfering (si)-UCA1 or overexpression (oeUCA1). GAPDH, glyceraldehyde-3-phosphate dehydrogenase. si-UCA1: small RNA interfering group; si-NC: without small interfering group.

angiogenesis. As HRECs cultured under high-glucose conditions were shown to mimic the pathogenesis of DR, the cells were also cultured under high-glucose (25 mmol/L) conditions. Likewise, the effect of UCA1-induced retinal endothelial cells angiogenesis under 5 mmol/L glucose was enhanced after 25 mmol/L glucose treatment. All of these results show that UCA1 can promote high-glucose-induced human retinal endothelial cells angiogenesis.

A new post-transcriptional regulatory mechanism has been identified; that is, that lncRNAs function as microRNA sponges to regulate gene expression<sup>37</sup>. LncRNA UCA1 can closely interact with miRNAs. For instance, UCA1 sponged miR-206 to exacerbate atherosclerosis events induced by oxidized low-density lipoprotein in THP-1 cells<sup>38</sup>. In addition, UCA1 can promote gefitinib resistance by sponging miR-143 in non-small cell lung cancer<sup>39</sup>. In addition, UCA1 functioned as a miRNA sponge to promote malignant phenotypes of renal cancer cells through sponging miR-182-5p<sup>40</sup>. In the present study, the expression levels of miR-624-3p in the plasma of DR patients and HRECs were found to be reduced, but UCA1 was increased. Thus, we speculated that UCA1 acted as a sponge of miR-624-3p. The miRNA sponge function of UCA1 is consistent with the evidence from the present study. First, the interaction between UCA1 and miR-624-3p was predicted using a bioinformatics database, which predicted that UCA1 contains a miR-624-3p binding site. Second, miR-624-3p downregulation efficiently reversed the inhibition effect by UCA1 siRNA.

Furthermore, miR-624-3p upregulation significantly reduced in the presence of UCA1. In addition, we found that UCA1 could pull down miR-624-3p. Finally, the present study also clearly identified a role for miR-624-3p in angiogenesis. The suppression of miR-624-3p expression essentially led to significant inhibition of the principal features of HRECs in DR progression, including proliferation, migration and angiogenesis.

It has been shown that expression and release of VEGF triggers deleterious vascular changes and leads to DR<sup>41</sup>. Clinical trial data showed that the improvement rates in the subgroup of patients with moderately severe or severe non-proliferative DR were greatly improved by inhibiting VEGF<sup>42</sup>. As an important member of the VEGF family, VEGF-C used to be a predominant tumor metastasis-driving factor in cancers<sup>43</sup>. We found that VEGF-C was elevated in DR patients, which was consistent with previous findings<sup>10</sup>. Herein, we predicted miR-624-3p to target the 3'UTR of VEGF-C using bioinformatics prediction tools, which was found to have a high binding affinity between miR-624-3p and VEGF-C by a dual-luciferase assay. *In vitro* experiments, we showed that UCA1 can target miR-624-3p and subsequently promote VEGF-C expression in retinal endothelial cells, especially under the high-glucose culture. This is an important study that provides evidence for the post-transcriptional regulation of VEGF-C controlled by UCA1 depending on miR-624-3p in high glucose-induced retinal endothelial cells.

In summary, we identified UCA1 as an important factor associated with DR, which plays a key role in retinal endothelial

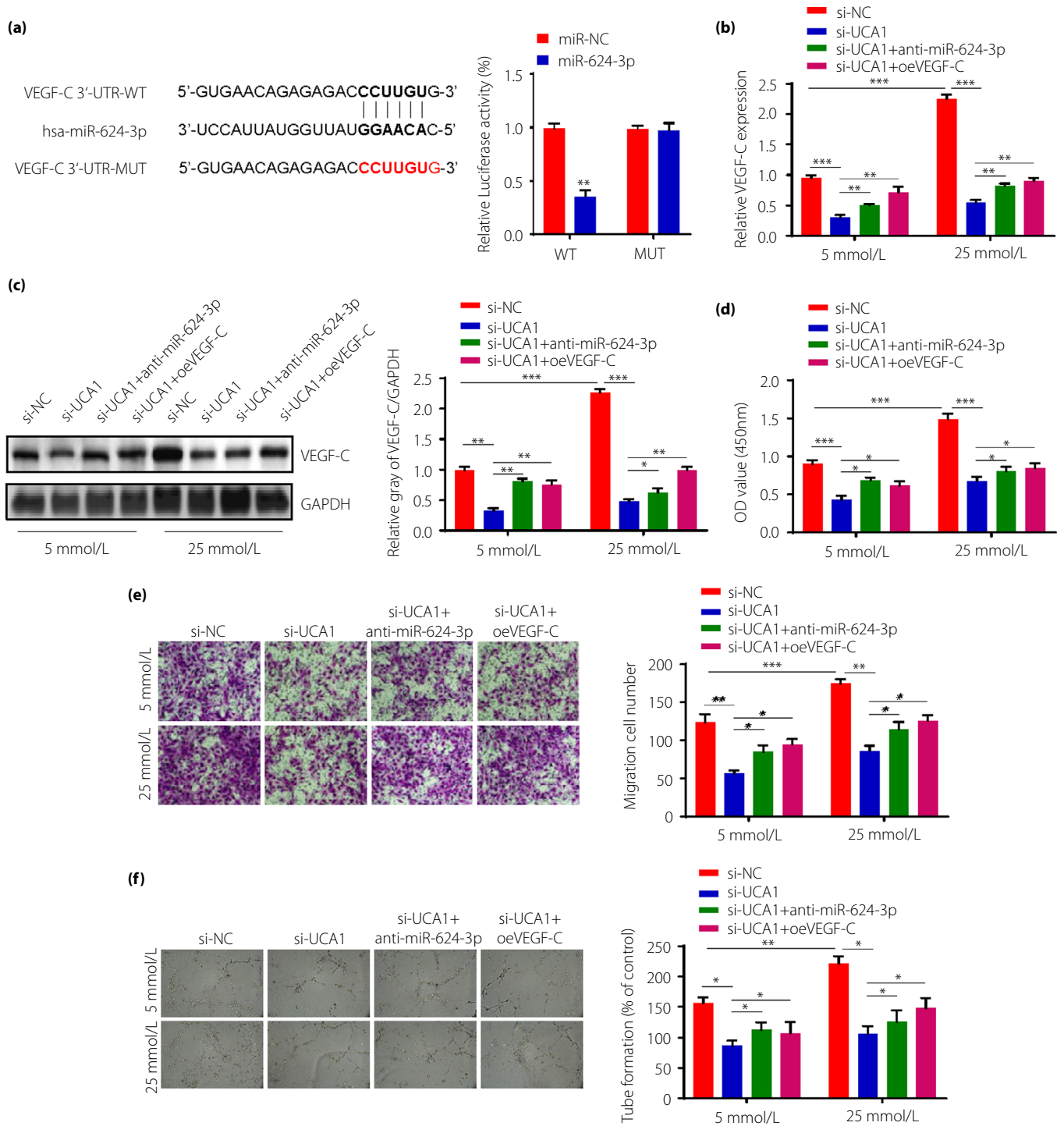


**Figure 4** | Urothelial carcinoma-associated 1 (UCA1) promoted high-glucose-induced human retinal endothelial cells proliferation, migration and angiogenesis through regulating micro-ribonucleic acid (miR)-624-3p/vascular endothelial growth factor V (VEGF-C). (a) Schematic showing the predicted miR-624-3p sites in VEGF-C and luciferase assays in wild-type (WT)-VEGF-C or mutant (MUT)-VEGF-C human retinal endothelial cells co-transfected with miR-NC or miR-624-3p. (b) The messenger ribonucleic acid expressions of VEGF-C were detected by reverse transcription polymerase chain reaction. (c) Protein levels of VEGF-C were detected by western blot. (d) Cell Counting Kit-8 assay was used to measure cell proliferation abilities. (e) Migration abilities were measured by Transwell assay. (f) Tube formation assay was carried out to detect cell angiogenesis ability. si-UCA1: small RNA interfering group; si-NC: without small interfering group. \* $P < 0.05$ , \*\* $P < 0.01$ , \*\*\* $P < 0.001$ .



cells angiogenesis. Furthermore, we report the interaction between UCA1 and miR-624-3p, and show that UCA1 regulates the expression of VEGF-C by sponging miR-624-3p in high-glucose-exposed human retinal endothelial cells (Figure S2). The present results pave the way for further studies on diagnostic and therapeutic studies related to UCA1 in DR patients.

## ACKNOWLEDGMENTS

We express our gratitude to all those who financed the study.

## DISCLOSURE

The authors declare no conflict of interest.

## REFERENCES

1. Yu DY, Cringle SJ, Su EN, *et al.* Pathogenesis and intervention strategies in diabetic retinopathy. *Clin Exp Ophthalmol* 2001; 29: 164–166.
2. Wan TT, Li XF, Sun YM, *et al.* Recent advances in understanding the biochemical and molecular mechanism of diabetic retinopathy. *Biomed Pharmacother* 2015; 74: 145–147.
3. Hendrick AM, Gibson MV, Kulshreshtha A. Diabetic retinopathy. *Prim Care* 2015; 42: 451–464.
4. Distler JH, Hirth A, Kurowska-Stolarska M, *et al.* Angiogenic and angiostatic factors in the molecular control of angiogenesis. *Q J Nucl Med* 2003; 47: 149–161.
5. Wang H, Xu X, Yin Y, *et al.* Catalpol protects vascular structure and promotes angiogenesis in cerebral ischemic rats by targeting HIF-1 $\alpha$ /VEGF. *Phytomedicine* 2020; 78: 153300.
6. Xu B, Zhang H, Zhu M, *et al.* Critical role of trophic factors in protecting müller glia: implications to neuroprotection in age-related macular degeneration, diabetic retinopathy, and Anti-VEGF therapies. *Adv Exp Med Biol* 2019; 1185: 469–473.
7. Faatz H, Rothaus K, Westhues D, *et al.* Treatment adherence and effectiveness of anti-Vascular Endothelial Growth Faktor (VEGF) treatment of diabetic macular edema in the clinical routine : comparison between cooperative and unicentric organization of treatment. *Ophthalmologie* 2020; 117: 557–565.
8. Ferrão J, Bonfim Neto AP, da Fonseca VU, *et al.* Vascular endothelial growth factor C treatment for mouse hind limb lymphatic revascularization. *Vet Med Sci* 2019; 5: 249–259.
9. Zhao JF, Hua HR, Chen QB, *et al.* Impact of fenofibrate on choroidal neovascularization formation and VEGF-C plus VEGFR-3 in Brown Norway rats. *Exp Eye Res* 2018; 174: 152–160.
10. Li Y, Chen D, Sun L, *et al.* Induced expression of VEGFC, ANGPT, and EFNB2 and their receptors characterizes neovascularization in proliferative diabetic retinopathy. *Investig Ophthalmol Vis Sci* 2019; 60: 4084–4096.
11. Liu Z, Chen Q, Hann SS. The functions and oncogenic roles of CCAT1 in human cancer. *Biomed Pharmacother* 2019; 115: 108943.
12. Li X, Wu Z, Fu X, *et al.* lncRNAs: insights into their function and mechanics in underlying disorders. *Mutat Res Rev Mutat Res* 2014; 762: 1–21.
13. Zhang C, Xie L, Liang H, *et al.* lncRNA MIAT facilitates osteosarcoma progression by regulating mir-128-3p/VEGFC axis. *IUBMB Life* 2019; 71: 845–853.
14. Yu C, Longfei L, Long W, *et al.* lncRNA PVT1 regulates VEGFC through inhibiting miR-128 in bladder cancer cells. *J Cell Physiol* 2019; 234: 1346–1353.
15. Zhang Z, Hao H, Zhang CJ, *et al.* Evaluation of novel gene UCA1 as a tumor biomarker for the detection of bladder cancer. *Zhonghua Yi Xue Za Zhi* 2012; 92: 384–387.
16. He Q, Meng J, Liu S, *et al.* Long non-coding RNA UCA1 upregulates KIF20A expression to promote cell proliferation and invasion via sponging miR-204 in cervical cancer. *Cell Cycle* 2020; 19: 2486–2495.
17. Gao Q, Fang X, Chen Y, *et al.* Exosomal lncRNA UCA1 from cancer-associated fibroblasts enhances chemoresistance in vulvar squamous cell carcinoma cells. *J Obstet Gynaecol Res* 2020; 47: 73–87.
18. Zhao X, Wang Y, He J, *et al.* lncRNA UCA1 maintains the low-tumorigenic and nonmetastatic status by stabilizing E-cadherin in primary prostate cancer cells. *Mol Carcinog* 2020; 59: 1174–1187.
19. Yu R, Zhang Y, Lu Z, *et al.* Long-chain non-coding RNA UCA1 inhibits renal tubular epithelial cell apoptosis by targeting microRNA-206 in diabetic nephropathy. *Arch Physiol Biochem* 2019; 12: 1–9.
20. Shi CH, Huang Y, Li WQ, *et al.* Influence of lncRNA UCA1 on glucose metabolism in rats with diabetic nephropathy through PI3K-Akt signaling pathway. *Eur Rev Med Pharmacol Sci* 2019; 23: 10058–10064.
21. Bak RO, Mikkelsen JG. miRNA sponges: soaking up miRNAs for regulation of gene expression. *Wiley Interdiscip Rev RNA* 2014; 5: 317–333.
22. Liang WC, Fu WM, Wong CW, *et al.* The lncRNA H19 promotes epithelial to mesenchymal transition by functioning as miRNA sponges in colorectal cancer. *Oncotarget* 2015; 6: 22513–22525.
23. Lin CY, Wang SW, Chen YL, *et al.* Brain-derived neurotrophic factor promotes VEGF-C-dependent lymphangiogenesis by suppressing miR-624-3p in human chondrosarcoma cells. *Cell Death Dis* 2017; 8: e2964.
24. Bertoli G, Cava C, Castiglioni I. MicroRNAs: new biomarkers for diagnosis, prognosis, therapy prediction and therapeutic tools for breast cancer. *Theranostics* 2015; 5: 1122–1143.
25. Dagher Z, Park YS, Asnaghi V, *et al.* Studies of rat and human retinas predict a role for the polyol pathway in human diabetic retinopathy. *Diabetes* 2004; 53: 2404–2411.
26. Yuan L, Hu J, Luo Y, *et al.* Upregulation of heparanase in high-glucose-treated endothelial cells promotes endothelial cell migration and proliferation and correlates with Akt and extracellular-signal-regulated kinase phosphorylation. *Mol Vis* 2012; 18: 1684–1695.

27. Chen X, Li J, Li M, *et al.* KH902 suppresses high glucose-induced migration and sprouting of human retinal endothelial cells by blocking VEGF and PlGF. *Diabetes Obes Metab* 2013; 15: 224–233.
28. Chen Z, Liu G, Xiao Y, *et al.* Adrenomedullin22-52 suppresses high-glucose-induced migration, proliferation, and tube formation of human retinal endothelial cells. *Mol Vis* 2014; 20: 259–269.
29. Yan C, Zhang Z, Bao S, *et al.* Computational methods and applications for identifying disease-associated lncRNAs as potential biomarkers and therapeutic targets. *Mol Ther Nucleic Acids* 2020; 21: 156–171.
30. Hu J, Gao Y, Li J, *et al.* A novel algorithm based on bi-random walks to identify disease-related lncRNAs. *BMC Bioinformatics* 2019; 20(Suppl 18): 569.
31. Shi Y, Chen C, Xu Y, *et al.* lncRNA FENDRR promotes high-glucose-induced proliferation and angiogenesis of human retinal endothelial cells. *Biosci Biotechnol Biochem* 2019; 83: 869–875.
32. Yang J, Yang FJ, Wang YG, *et al.* lncRNA MIR497HG inhibits proliferation and migration of retinal endothelial cells under high-level glucose treatment via miRNA-128-3p/SIRT1 axis. *Eur Rev Med Pharmacol Sci* 2020; 24: 5871–5877.
33. Expression of Concern. Phycion 8-O- $\beta$ -glucopyranoside exerts protective roles in high glucose-induced diabetic retinopathy via regulating lncRNA NORAD/miR-125/STAT3 signalling. *Artif Cells Nanomed Biotechnol* 2020; 48: 705.
34. Gong Q, Dong W, Fan Y, *et al.* lncRNA TDRG1-mediated overexpression of VEGF aggravated retinal microvascular endothelial cell dysfunction in diabetic retinopathy. *Front Pharmacol* 2019; 10: 1703.
35. Sun Y, Liu YX. lncRNA HOTTIP improves diabetic retinopathy by regulating the p38-MAPK pathway. *Eur Rev Med Pharmacol Sci* 2018; 22: 2941–2948.
36. Zhang D, Qin H, Leng Y, *et al.* lncRNA MEG3 overexpression inhibits the development of diabetic retinopathy by regulating TGF- $\beta$ 1 and VEGF. *Exp Ther Med* 2018; 16: 2337–2342.
37. Salmena L, Poliseno L, Tay Y, *et al.* A ceRNA hypothesis: the Rosetta Stone of a hidden RNA language. *Cell* 2011; 146: 353–358.
38. Hu X, Ma R, Fu W, *et al.* lncRNA UCA1 sponges miR-206 to exacerbate oxidative stress and apoptosis induced by ox-LDL in human macrophages. *J Cell Physiol* 2019; 234: 14154–14160.
39. Chen X, Wang Z, Tong F, *et al.* lncRNA UCA1 promotes gefitinib resistance as a ceRNA to target FOSL2 by sponging miR-143 in non-small cell lung cancer. *Mol Ther Nucleic Acids* 2020; 19: 643–653.
40. Wang W, Hu W, Wang Y, *et al.* Long non-coding RNA UCA1 promotes malignant phenotypes of renal cancer cells by modulating the miR-182-5p/DLL4 axis as a ceRNA. *Mol Cancer* 2020; 19: 18.
41. Rossino MG, Lulli M, Amato R, *et al.* Oxidative stress induces a VEGF autocrine loop in the retina: relevance for diabetic retinopathy. *Cells* 2020; 9: 1452.
42. Singh RP, Elman MJ, Singh SK, *et al.* Advances in the treatment of diabetic retinopathy. *J Diabetes Complications* 2019; 33: 107417.
43. Lu JM, Zhang ZZ, Ma X, *et al.* Repression of microRNA-21 inhibits retinal vascular endothelial cell growth and angiogenesis via PTEN dependent-PI3K/Akt/VEGF signaling pathway in diabetic retinopathy. *Exp Eye Res* 2020; 190: 107886.

## SUPPORTING INFORMATION

Additional supporting information may be found online in the Supporting Information section at the end of the article.

**Figure S1** | The expression of other vascular endothelial growth factor subtypes in long non-coding ribonucleic acid urothelial carcinoma-associated 1-regulated human retinal endothelial cells.

**Figure S2** | The diagram schematically illustrating our findings

**Table S1** | Micro-ribonucleic acid correlations with long non-coding ribonucleic acid urothelial carcinoma-associated 1.